Theory of Batchwise Centrifugal Filtration

In centrifugal filtration, centrifugal forces serve as the driving force in the production of cakes. Centrifugal sedimentation leads to formation of a clear supernatant followed by a slurry and a cake that grows and compacts simultaneously. The slurry concentration is independent of radius but decreases everywhere within the suspension at the same rate with respect to time. The theoretical analysis of centrifugal filtration presented here takes cake compressibility and variable permeability into account. Experiments were carried out under low driving forces with a centrifuge having a diameter of 150 mm and speeds of 1,000-2,000 RPM. With centrifugal accelerations of 75-300 g and pressure differentials under 1 atm, the sedimentation process was relatively slow and could be observed experimentally with ease.

Masao Sambuichi, Hideo Nakakura, Kunihisa Osasa
Yamaguchi University
Ube, Japan 755

F.M. Tiller
University of Houston
Houston, TX 77004

Centrifugal Filtration and Sedimentation

Centrifugal sedimentation and centrifugal filtration are carried out in solid-bowl, Figure 1, and perforated-bowl, Figure 2, centrifuges. In batch centrifugal sedimentation, three interfaces are produced. The first involves gas and liquid, the second supernatant clear liquid and the slurry surface, while the third appears as the interface between slurry and cake. As the solids sediment out of the slurry, they form a network of interconnected particles capable of sustaining compressive and shear forces. In the suspension, particles are not in contact and cannot transmit internal forces from one to another. Once a structure is formed in the cake zone, it undergoes a compression process in which liquid is squeezed out of the sediment until the structure is sufficiently consolidated to carry the forces produced by the centrifuge.

The thickness of the sediment for centrifugal sedimentation is less than for a gravitational process because the increased acceleration produces larger compressive forces. In centrifugal filtration, liquid passes through the cake and the supporting medium, which may be paper, cloth, metal screen, or any porous material. In contrast to centrifugal sedimentation, a density difference between liquid and solid is not necessary for operation.

In Figure 3a gravity and centrifugal sedimentation are compared. In gravity sedimentation, the upper interface initially falls at a constant rate along H_oA. Simultaneously, sediment forms at the bottom of the container and the settling velocity decreases. The slurry begins to concentrate at successively greater distances from the bottom, and ultimately when the upper interface reaches A it begins to fall at a slower pace. At B the rising sediment meets the upper interface and the slurry disappears, leaving all of the solids in the sediment or cake. Further consolidation results from disruption of the particulate structure in a squeezing process. The velocity and flux of particles is generally assumed to be a unique function of concentration up to point B, or point B' in centrifugal sedimentation. After B or B' is reached, expression of liquid under gravitational or centrifugal action is controlled by Darcian-type equations (Tiller, 1981).

Batchwise centrifugal sedimentation and filtration are compared in Figure 3b. As liquid flows through the cake, the level of the liquid decreases and the cake builds up faster than in pure sedimentation. Because the centrifugal forces are the same in the two processes, the heights of the final sediments are approximately equal.

Development of a theoretical structure for centrifugal filtration requires consideration of both the sedimenting and cake filtration portions of the process. Although there is an extensive literature on practical aspects of centrifugation, there is no rigorous treatment of centrifugal filtration of compressible cakes. Mathematical analyses of the ultracentrifuge used for obtaining molecular masses of macromolecules have long been available (Fujita, 1962). Grace (1953) published an extensive analysis of the compression-permeability (C-P) cell in relation to constant-pressure filtration and centrifugal filtration. He employed the C-P cell to obtain porosity ϵ and specific flow resistance α as functions of effective or compressive drag pressure p_s, which were then used to solve the differential equations of constant-pressure and centrifugal filtration, yielding filtrate volume as a function of time. Although he obtained excellent agreement between experimental filtration data and calculations based on C-P cell results, current opinion (Tiller and Leu, 1980; Willis and Tosun, 1980; Shirato, 1983) does not favor the cell as an accurate means for providing data for constitutive relationships.

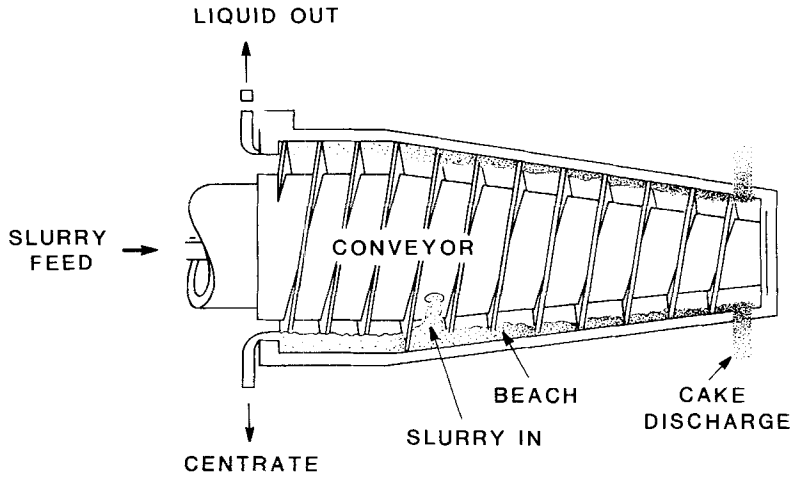

CENTIFUGAL SEDIMENTOR

Figure 1. Sedimenting centrifuge.

Grace (1953) developed approximate solutions for centrifugation. However, he concluded that rigorous values of average specific flow resistance could not be calculated with only C-P cell data. He assumed that it was necessary to have the effective pressure as a function of the variable cake radius but did not suggest how such information could be obtained. We shall show how it is possible to calculate p_s as a function of r.

Oyama and Sumikawa (1954) recognized that specific resistances obtained in centrifugal filtration were larger than those of constant-pressure filtration when liquid pressure drops were the same in the two processes. Valleroy and Malony (1960) reported differences of 20% in average resistances.

Most investigators have neglected the effect of sedimentation during the centrifugation process. Hultsch and Wilkesmann (1977) suggested testing procedures in which a cake first formed in a vacuum filter is transferred to a bucket centrifuge. Rates of flow are then determined for different rotational speeds and cake thicknesses. It is frequently assumed that the sedimentation period occurs very rapidly and that then the clear supernatant liquid flows through the cake. We shall analyze all phases of the centrifugal filtration process. Straumann (1963) developed nondimensional equations involving simultaneous settling and filtration. Sambuichi et al. (1982) derived equations for cake growth in constant-pressure filtration that included particulate sedimentation.

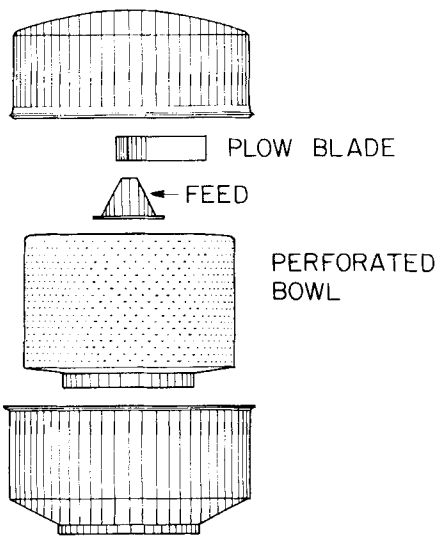

CENTRIFUGAL FILTER

Figure 2. Filtering centrifuge.

Centrifugal Sedimentation Theory

The rate of cake buildup in a batch centrifugal filter depends upon the solid flux at the cake surface. The velocity of the solids at the interface of the cake and slurry is the sum of the velocity of the liquid due to filtrate flow and the superimposed centrifugal settling velocity. A general three-dimensional view of conditions in the slurry and sediment (cake) is provided in Figure 4. Initially the concentration in the sediment is assumed to be constant and equal to ϕ_{sF}. As time continues, the concentration drops with time in accord with Eq. 14. The solids settle more rapidly than the liquid, and cake is formed on the perforated bowl of the centrifuge. Three regions, consisting of supernatant liquid, settling particles in the slurry, and cake appear in the first phase (AB in Figure 4). After the particulates completely settle out, the second phase consisting of supernatant liquid and cake is entered (BC). Liquid passes through the cake of fixed mass of solids which is simultaneously being reduced in thickness. In some commercial designs (Lilley and Hultsch, 1975), the liquid is siphoned out of the centrifuge at this stage so that it does not have to pass through the cake. In the final stage (which we do not consider) liquid is centrifugally drained from the cake, resulting in two-phase flow of gas and liquid.

The volume fraction of solids, ϵ_s, in the cake is shown in Figure 4 to vary with depth of sediment in. The concentration at the

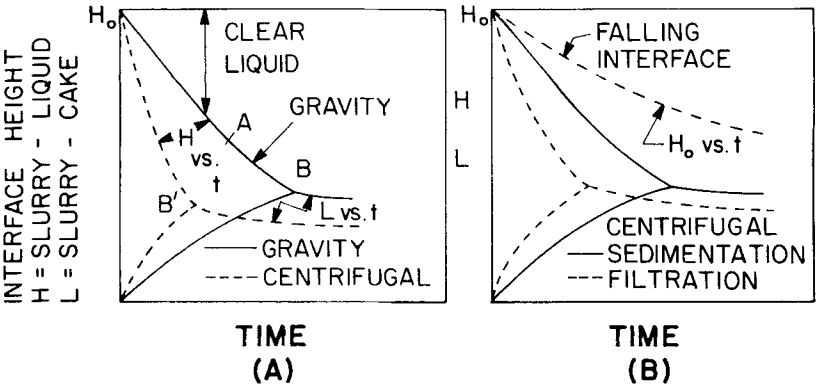

Figure 3a. Gravitational and centrifugal sedimentation.

Figure 3b. Batchwise centrifugal sedimentation and filtration.

cake surface, ϵ_{so}, is assumed to remain constant while the value of ϵ_s in contact with the supporting centrifuge surface increases with time as the cake thickness increases. We turn first to centrifugal sedimentation theory.

We wish to follow the radii vs. time of the interface of the gas and supernatant liquid r_L, the interface of the supernatant and slurry r_s, and the radius of the cake r_c, shown in Figure 5. All three radii depend upon phenomena related to both sedimentation and Darcian flow in the cake.

We shall assume that centrifugal sedimenting velocities of solids relative to the liquid can be obtained from gravitational experiments through a ratio of the accelerations. In gravitational sedimentation experiments in a cylinder, the volumetric flux of solids down exactly balances the upward liquid flux

$$u\phi + u_g\phi_s = 0 \tag{1}$$

where u_g is the observed velocity downward under gravity, and ϕ and ϕ_s are respectively the average volumetric fractions of liquid and solid. Solving for u in Eq. 1, subtracting from u_g, and noting that $\phi + \phi_s = 1$ leads to the relative velocity

$$u_g - u = u_g/\phi \tag{2}$$

The liquid and solid velocities have opposite signs in gravitational sedimentation. Our interest lies in the absolute value of u_g/ϕ.

In centrifugal filtration, the liquid flows in the same direction as the solids due to the production of filtrate. The sum of the solid and liquid fluxes at radius r equals the filtrate flux exiting from the perforated bowl in accord with

$$2\pi r(u\phi + u_c\phi_s) = 2\pi r_o u_o \tag{3}$$

where u_c = centrifugal sedimenting velocity, r_o = centrifuge radius, and u_o = filtrate velocity. Solving for u in Eq. 3 and subtracting from u_c yields the relative velocity

$$u_c - u = \frac{u_c}{\phi} - \frac{u_o r_o}{r\phi} \tag{4}$$

We make the ratio of Eq. 4 to Eq. 2 equal to $r\omega^2/g$ and solve for u_c to obtain

$$u_c = \frac{r\omega^2}{g}u_g + \frac{u_o r_o}{r} \tag{5}$$

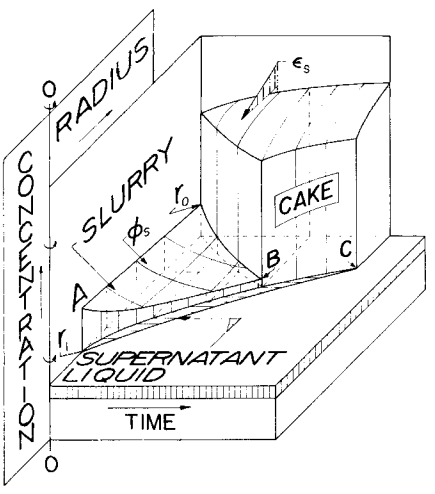

Figure 4. Three-dimensional view of conditions in slurry and sediment.

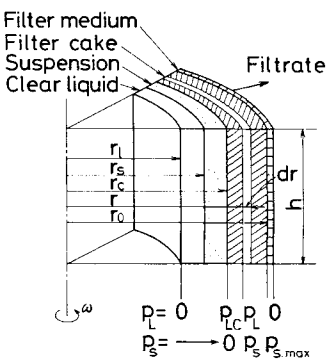

Figure 5. Schematic diagram in a centrifugal basket.

Equation 5 can be expected to be valid as long as the Reynolds number does not increase to the point that the sedimentation characteristics change.

Centrifugal sedimentation, with its radial flow, differs from gravitational sedimentation in two important aspects. The acceleration and area are both proportional to the radius. Thus even with a uniform slurry the particle flux is not constant, and the resulting equations are more complex than those applying to simple gravitational sedimentation. Equating the rate of change of flux across radius r to the rate of increase (actually a decrease) of solid in the region r to $r + dr$ yields

$$d(2\pi r u_c \phi_s) + 2\pi r \frac{\partial \phi_s}{\partial t} dr = 0 \tag{6}$$

Assuming u_c to be given by Eq. 5, we obtain

$$\frac{\partial}{\partial r}\left[\left(\frac{r^2\omega^2}{g} u_g + r_o u_o\right)\phi_s\right] + r\frac{\partial \phi_s}{\partial t} = 0 \tag{7}$$

Equations 6 and 7 must be modified if diffusional forces due to Brownian motion are present. We shall assume that centrifugal forces predominate.

It is generally assumed that the settling velocity u_g is a unique function of the volume fraction ϕ_s of solids in the slurry (Kynch, 1952; Wakeman and Holdrich, 1982). On that basis, Eq. 7 is modified into the form

$$\left[\frac{r^2\omega^2}{g}\frac{d}{d\phi_s}(u_g\phi_s) + r_o u_o\right]\frac{\partial \phi_s}{\partial r} + r\frac{\partial \phi_s}{\partial t} + \frac{2r\omega^2}{g} u_g \phi_s = 0 \tag{8}$$

When the initial concentration ϕ_{sF} is uniform, we shall demonstrate that ϕ_s remains independent of r over that portion of the slurry which is unaffected by the rising cake. At $t = 0$, the flux of solids in at r_1 minus the flux out at r_2 yields the net flux as follows

$$\begin{aligned}\text{net flux} &= 2\pi r_1\left(\frac{r_1\omega^2}{g} u_g + \frac{r_o u_o}{r_1}\right)\phi_s \\ &\quad - 2\pi r_2\left(\frac{r_2\omega^2}{g} u_g + \frac{r_o u_o}{r_2}\right)\phi_s \end{aligned} \tag{9}$$

$$= 2\pi\frac{\omega^2}{g} u_g (r_1^2 - r_2^2)\phi_s \tag{10}$$

This value is negative as $r_2 > r_1$. Initially the volume of particles in the centrifuge between r_1 and r_2 is $\pi(r_2^2 - r_1^2)\phi_s$. Dividing the volume of solids by the net flux yields the rate at which solids are depleted

$$\text{rate} = -\frac{2\omega^2}{g} u_g \tag{11}$$

which is independent of r. Near the surface of the cake that is building up, other conditions exist which for this investigation we shall assume to be negligible. If ϕ_s is independent of r, Eq. 8 reduces to (Kamac, 1951; Brown, 1970)

$$\frac{d\phi_s}{dt} + \frac{2\omega^2}{g} u_g \phi_s = 0 \tag{12}$$

We assume that the flux $u_g\phi_s$ is a unique function of ϕ_s, which necessitates operation in a zone settling region. In Figure 6 a plot of the settling velocity is shown for $CaCO_3$ in the range of ϕ_s used for experimentation in this investigation. We assume that the settling flux is restricted to the linear region in which

$$u_g\phi_s = c_1 - c_2\phi_s \tag{13}$$

Inserting this relation in Eq. 12 and integrating yields

$$\phi_s = \frac{c_1}{c_2} - \left(\frac{c_1}{c_2} - \phi_{sF}\right)e^{2c_2\omega^2 t/g} \tag{14}$$

This value of ϕ_s is valid for $r_s < r < r_c$. For the region in which $r_L < r < r_s$, ϕ_s has a value of zero.

The radius r_L of the supernatant liquid can be obtained from a simple volumetric balance relating the volume of filtrate to the reduction in volume of the contents of the centrifuge as follows

$$r_L^2 = r_F^2 + 2r_o\int_o^t u_o\, dt \tag{15}$$

The velocity of the slurry interface is given by Eq. 5 where r_s replaces r

$$u_s = \frac{dr_s}{dt} = \frac{dr_s}{d\phi_s}\frac{d\phi_s}{dt} = \frac{r_o}{r_s} u_o + \frac{r_s\omega^2}{g} u_g \tag{16}$$

Eliminating $d\phi_s/dt$ by means of Eq. 12 and rearranging terms leads to

$$\frac{d}{d\phi_s} r_s^2 + \frac{r_s^2}{\phi_s} = -\frac{g}{\omega^2}\frac{r_o u_o}{u_g\phi_s} \tag{17}$$

Integration yields a relation between r_s and ϕ_s as follows:

$$\phi_s r_s^2 - \phi_{sF} r_F^2 = \frac{g r_o}{\omega^2}\int_{\phi_s}^{\phi_{sF}} \frac{u_o}{u_g} d\phi_s \tag{18}$$

$$= 2r_o\int_o^t u_o\phi_s\, dt \tag{19}$$

where the variable on the righthand side has been changed back

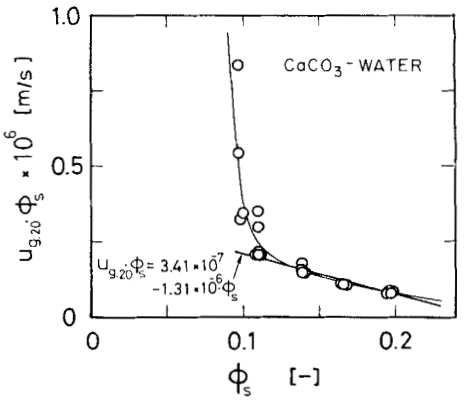

Figure 6. Settling flux at 20°C.

to t. The concentration ϕ_s can be expressed as a function of t by means of Eq. 14.

When high centrifugal speeds are combined with large specific gravity differences, the slurry interface will rapidly disappear, leaving the liquid to flow through the compacted cake. With neutrally buoyant particles, the gravitational settling velocity $u_g = 0$, and $r_L = r_s$. Between these two extremes, many possibilities exist.

Cake Formation

Having obtained expressions for the radial positions of the liquid and slurry interfaces, we turn to the radius r_c of the cake. Whereas the time derivatives of r_L and r_s are positive, dr_c/dt is negative. A rate balance over a portion of the centrifuge between an arbitrary radius r lying in the slurry and r_o takes the form

$$2\pi r\phi_s\left(\frac{r\omega^2}{g}u_g + \frac{r_o u_o}{r}\right) = \frac{d}{dt}\left(\pi\phi_s(r_c^2 - r^2)\right] + \frac{d}{dt}\left[\pi\epsilon_{sav}(r_o^2 - r_c^2)\right] \quad (20)$$

where the average solidosity of the cake is defined by

$$\epsilon_{sav} = \int_{r_c}^{r_o} 2r\epsilon_s\, dr/(r_o^2 - r_c^2) \quad (21)$$

Differentiating the righthand side of Eq. 20 and simplifying yields

$$2\left(\frac{r^2\omega^2}{g}u_g\phi_s + r_o u_o\phi_s\right) = (r_c^2 - r^2)\frac{d\phi_s}{dt} + 2\phi_s r_c\frac{dr_c}{dt} + \frac{d}{dt}\left[\epsilon_{sav}(r_o^2 - r_c^2)\right] \quad (22)$$

When $r = r_c$, the equation describes conditions at the cake surface as follows

$$2\pi r_c\left(\frac{r_c\omega^2}{g}u_g + \frac{r_o u_o}{r_c}\right)\phi_s = \frac{d}{dt}\left[\epsilon_{sav}(r_o^2 - r_c^2)\right] + 2\phi_s r_c\frac{dr_c}{dt} \quad (23)$$

The second term on the righthand side represents the particulates in the slurry contained in $2\pi r_c\, dr_c$ (dr_c is negative) and swallowed up by the expanding cake. The righthand side of Eq. 23 is multiplied by $dt/d\phi_s$. The lefthand side is multiplied by $-g/2\omega^2 u_g\phi_s$, which equals $dt/d\phi_s$ based on Eq. 12. Then Eq. 23 becomes

$$\frac{d}{d\phi_s}\left[\epsilon_{sav}(r_o^2 - r_c^2)\right] + \phi_s\frac{dr_c^2}{d\phi_s} = -r_c^2 - \frac{r_o g u_o}{\omega^2 u_g} \quad (24)$$

Combining the second and third terms into $d(\phi_s r_c^2)/d\phi_s$ and rearranging

$$d\left[(\epsilon_{sav} - \phi_s)r_c^2 - \epsilon_{sav}r_o^2\right] = \frac{r_o g}{\omega^2}\frac{u_o}{u_g}d\phi_s \quad (25)$$

at $t = 0$, $\phi_s = \phi_{sF}$, $r_c = r_o$, and $\epsilon_{sav} = \epsilon_{so}$. Integrating and substituting limits yields the relation between r_c and ϕ_s

$$r_c^2(\epsilon_{sav} - \phi_s) - r_o^2(\epsilon_{sav} - \phi_{sF}) = \frac{r_o g}{\omega^2}\int_{\phi_{sF}}^{\phi_s}\frac{u_o}{u_g}d\phi_s \quad (26)$$

Time can be introduced by relating ϕ_s to t through Eq. 14.

Equations 15, 19, and 26 provide relations for r_L, r_s, r_c as functions of t or ϕ_s. The filtrate rate u_o and the average volume fraction of solids ϵ_{sav} in the cake must be known before the position of the interfaces can be calculated. They can be calculated theoretically by solving the appropriate flow equations or through experiment. The quantity u_g can be obtained as a function of ϕ_s from gravitational settling experiments.

We next consider flow through the cake.

Force Balance

A momentum balance reduces to a simple force balance when the inertial terms are neglected. A force balance over a differential element is required to relate the effective or compressive pressure p_s to the hydraulic pressure p_L. Cakes are similar to soils, and a lateral stress is developed which we assume to be proportional to the normal stress on the particles. If F_s is the stress/height on the particles between the cake radius r_c and an arbitrary radius r, the effective pressure developed by the accumulative frictional drag is defined by

$$p_s = F_s/2\pi r \quad (27)$$

The lateral stress orthogonal to a radius vector is given by $k_o F_s$. Assuming momentum changes to be negligible and utilizing Figure 7, a force balance yields

$$d(rp_L)\mathrm{d}\theta + d(rp_s)d\theta - (p_L + k_o p_s)dr\sin d\theta = [\rho\epsilon + \rho_s(1 - \epsilon)]\, r^2\omega^2 dr d\theta \quad (28)$$

where point contact among particles is assumed so that the liquid pressure is effective over the entire cross-sectional area. Assuming $d\theta = \sin d\theta$, Eq. 28 becomes (Shirato and Aragaki, 1969)

$$\frac{\partial p_L}{\partial r} + \frac{\partial p_s}{\partial r} + (1 - k_o)\frac{p_s}{r} - (\rho\epsilon + \rho_s\epsilon_s)r\omega^2 = 0 \quad (29)$$

The value of k_o generally ranges from 0.4 to 0.7, although higher values have been reported for clay (Dunn et al., 1980).

Flow Rate Equations in Spatial Coordinates

Darcy's law can be placed in either spatial or material coordinate form. The change in hydraulic pressure depends on the difference of the increasing centrifugal pressure and the decrease due to frictional losses. In spatial coordinates

$$\frac{\partial p_L}{\partial r} - \rho r\omega^2 = -\frac{\mu q}{K} = -\frac{\mu}{K}\frac{Q}{2\pi r} \quad (30)$$

where q = flow rate/unit height. The corresponding equation in material coordinates is unwieldy and will not be used in the initial development. Equations 29 and 30 are simultaneous equations in p_L, p_s, and r. Assumption of a quasi-steady state and

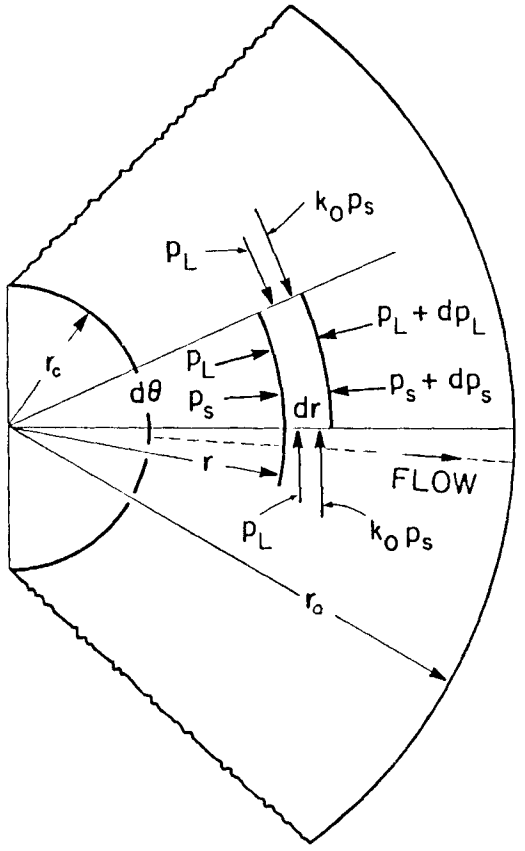

Figure 7. Force balance in a centrifugal filter cake.

constancy with respect to r of the overall liquid flow rate permits Eqs. 29 and 30 to be treated as ordinary differential equations.

The porosity ϵ, solidosity ϵ_s, and permeability K are functions of p_s. Consequently dp_L/dr must be eliminated between Eqs. 29 and 30 to give the following equation involving ϵ_s, K, p_s, and r

$$\frac{\partial p_s}{\partial r} + (1 - k_o)\frac{p_s}{r} - (\rho_s - \rho)\epsilon_s r\omega^2 = \frac{\mu}{K}\frac{Q}{2\pi r} \tag{31}$$

where Q is the flow rate per unit height at radius r in the cake, Q is a function of r and t, and partial derivatives should be employed in Eq. 31.

We next turn to the law of continuity. A material balance over the liquid in a differential portion of the cake can be written as

$$\frac{\partial}{\partial r}(rq) + r\frac{\partial \epsilon}{\partial t} = 0 \tag{32}$$

Combining this equation with Eqs. 29 and 30 leads to partial differential equatinos. However, if we assume the existence of quasi-steady state conditions in which $\partial\epsilon/\partial t$ is very small and $q = q(t)$, Eq. 32 can be replaced by

$$Q/2\pi = rq = r_o u_o \tag{33}$$

where r_o = centrifuge radius and u_o = filtrate volume/(unit height) (unit time). Combining Eqs. 31 and 33 yields the following ordinary differential equation where the filtration rate u_o is a function of time

$$\frac{dp_s}{dr} + (1 - k_o)\frac{p_s}{r} - (\rho_s - \rho)\epsilon_s r\omega^2 = \frac{\mu}{K}\frac{r_o u_o}{r} \tag{34}$$

This equation must be solved first to establish the effective pressure, p_s, as a function of r. When p_s is obtained, the cake structure is defined because K and ϵ_s are then known functions of r. Substitution of K and ϵ_s as functions of r at a given time in Eq. 30 permits direct integration for p_L as a function of r. In general, a trial and error process is required to satisfy boundary conditions.

Pressures at the Cake Boundaries

The filtration process must be divided into two stages. In the first stage both supernatant liquid and slurry are present. In the second stage all of the particles have been deposited, and only clear liquid remains outside of the cake. Solution of the differential equations involving liquid and effective pressures requires knowledge of their values at the cake surface and at the interface between the cake and the medium covering the inside of the perforated bowl. The liquid pressure at the surface of the cake is due to the pressure generated by the supernatant liquid and the slurry above the cake surface. It is given by

$$p_{Lc} = \frac{\omega^2}{2}[\rho(r_s^2 - r_L^2) + \rho_{sL}(r_c^2 - r_s^2)] \tag{35}$$

where the density of the slurry $\rho_{sL} = \rho(1 - \phi_s) + \rho_s\phi_s$. When the slurry disappears the pressure is given by $\omega^2\rho(r_c^2 - r_L^2)/2$. The liquid pressure rises as it enters the cake and then falls due to frictional losses to a value p_1 required to overcome the medium resistance, which is given by

$$p_1 = \mu u_o R_m \tag{36}$$

The pressure drop over the cake and medium is

$$\Delta p_L = \Delta p_c + \Delta p_m = \frac{\omega^2}{2} \cdot [\rho(r_s^2 - r_L^2) + \rho_{sL}(r_c^2 - r_s^2) + \rho(r_o^2 - r_c^2)] \tag{37}$$

The effective pressure at the surface of the cake is zero. Stress on the particulate structure builds up in accord with Eq. 34 as the liquid flows through the cake, and p_s reaches a maximum with respect to distance at $r = r_o$. At $t = 0$, all the pressure drop is absorbed by the medium, and $\Delta p_c = \Delta p_m$. As the cake builds up, the pressure drop across the cake increases and Δp_m decreases. Simultaneously, the values of r_L and r_s are decreasing, and the overall pressure drop decreases. The pressure drop, Δp_c, goes through a maximum. Consequently, at a fixed point in the cake the effective pressure may reach a maximum at some instant of time. Wherever that happens, the cake no longer changes structure, as both ϵ_s and K are functions of the maximum effective pressure. The mathematical solutions must then be modified to account for the irreversibility.

Before the various equations can be solved, constitutive relations involving K, ϵ_s, and p_s must be introduced and the values of the gravitational settling parameters determined.

Constitutive Equations

Experiments were performed with $CaCO_3$ ($\rho_s = 2{,}710$ kg/m^3) in both water and water-glycerine ($\rho = 1{,}111$ kg/m^3; $\mu = 4.06$ mPa · s) suspensions. Concentrations were chosen so that experiments would fall in the linear region in Figure 5, where values of concentrations varied from 0.112 to 0.197. The gravitational sedimentation velocity u_g was determined experimentally as a function of the slurry concentration ϕ_s in a 56 mm ID tube using an initial height of 80–150 mm (Sambuichi et al., 1980). The data were linearized in accord with Eq. 13. Values of $c_1 = 3.41 \times 10^{-7}$ m/s and $c_2 = 1.31 \times 10^{-6}$ m/s were obtained for water at 20°C. These values were modified for the water-glycerine experiments.

Local specific flow resistance α was obtained as a function of p_s utilizing:

1. The compression-permeability cell method (Ruth, 1946; Grace, 1953; Tiller et al., 1972) in the range of 15–280 kPa, and

2. settling experiments in the range of 0.001–2 kPa.

The procedure for the settling experiments depends upon obtaining the rate of formation of cake for very concentrated slurries at $t = 0$, calculating the rate of squeezing out of liquid, and estimating a value for the hydraulic pressure gradient. The value of the permeability, K, was then calculated using Darcy's law (Shirato et al., 1970). The data were represented by conventional formulas. Above a pressure of 23.5 Pa, power functions of p_s were used for α and $\epsilon = 1 - \epsilon_s$ as follows:

$$\alpha = 5.46(10^9)p_s^{0.364}\text{m/kg} \quad \epsilon = 0.934p_s^{-0.057} \tag{38}$$

Below 23.5 Pa, the flow resistance and porosity were assumed to be constant and to have values of $\alpha = \alpha_i = 1.72 \times 10^{-10}$ m/kg and $\epsilon = \epsilon_i = 0.78$. The permeability can be obtained from the relation

$$K = 1/\rho_s\alpha(1 - \epsilon) \tag{39}$$

Although the compression-permeability (C-P) method is known to have serious deficiencies (Risbud, 1974) and some authors prefer to obtain relations between local α and p_s using values of α_{av} vs. Δp_c as obtained from conventional filtration tests (Tiller and Leu, 1980), we chose to use a combination of data obtained from a C-P cell and settling of concentrated slurries. No current method is free of defects. Conventional filtration and capillary suction methods are seriously affected by sedimentation. The C-P cell suffers from wall friction. Flow through fixed beds is subject to migration and deposition of fine particles. In addition, the actual separation process may not be carried out in the same manner as the test program. Correlation of laboratory data with large centrifuge or filter data is a difficult task that has not been solved satisfactorily.

Experimental Methods

In order to illustrate the basic phenomena of sedimentation plus filtration, a centrifuge was operated at relatively low acceleration, $g = 75$–300, with pressures under 25 kPa. At high g, the particles rapidly sediment and it is difficult to follow the slurry interface. Conditions were such that the interface r_s could be observed for about two minutes.

The experimental apparatus is illustrated schematically in Figure 8. The filter basket (0.15 m ID and height of 0.083 m) was covered with a stainless steel sieve having 1.68 mm (JIS) openings. Toyo filter paper, No. 4, was used as a medium for cake support. The basket rotated in a horizontal plane with a vertical axis and was covered by a transparent plate.

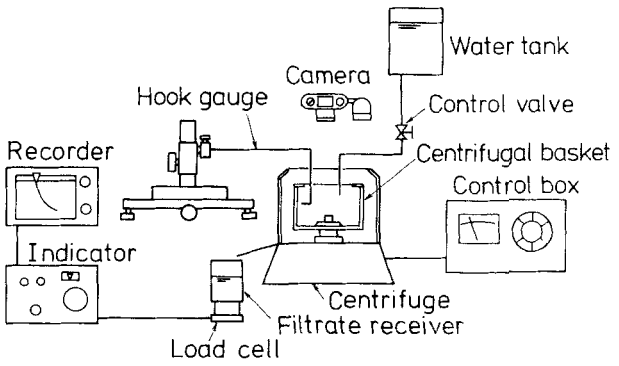

Figure 8. Experimental apparatus.

The batch feed consisted of 500 mL of slurry. Speeds of 1,000–2,000 RPM were maintained by a controller. Radii of the surface of the clear liquid r_L and the interface with the slurry r_s were measured with stroboscopic photography. The surface of the cake at r_c was not visible during the experiment, and r_c had to be calculated. The final cake radius was measured by the hook gauge at several points after completion of a run.

After completion of cake formation and determination of volume vs. time data, pure liquid was introduced and the average permeability was determined with a constant centrifugal pressure. Constant-pressure filtrations with the same slurries were performed in conventional equipment in order to compare characteristics of the filter cakes in centrifugal and standard constant-pressure filtrations. The medium resistance was measured with water permeation tests. These values were used in calculations even though they were probably less than the true resistance. The medium resistance was much smaller than the cake resistance in our work.

Determination of the particle size distribution of the $CaCO_3$ by the Andreasen pipette method led to the following Stokes diameters:

Microns	0–1	1–2	2–5	5–10	10–20	>20
Percent	11	12	34	28	9	6

Calculations

We shall employ a combination of experimental data and theoretically calculated values in analysis of centrifugal filtration. Basically we wish to predict the radii of the liquid, r_L; the interface with the slurry, r_s, and the cake surface, r_c; the average cake porosity; and the slurry composition as functions of time. The following procedure is used:

1. r_L is directly related to the volume of filtrate.

2. ϕ_s in the slurry layer is calculated as a function of time using Eq. 14.

3. r_s vs. t is obtained by a numerical integration of Eq. 16 where $dr_s = u_s dt$.

4. A p_s distribution and u_o are assumed, and ϵ and α or K obtained as functions of r using Eq. 34 and the compression-permeability cell and settling data.

5. The p_L distribution is found by using Eq. 30 subject to boundary conditions given by Eq. 36 for p_1 and Eq. 37 for Δp_L.

6. A new p_s-distribution is calculated from Eq. 34 and compared with the assumed distribution in step 4. The process is repeated until a satisfactory match has been obtained.

7. As a part of the iterative process on p_s, ϵ_{sav} is calculated, and r_c is obtained from Eq. 26 after substituting the assumed values of u_o and calculated values of σ_s from step 2.

Cake compression is neary irreversible, and it is generally assumed that the porosity and permeability are functions of the maximum value of the compressive pressure, p_s, reached with respect to material coordinates. In batch centrifugal filtration with diminution of the level of the liquid, the compressive pressure decreases with time. Consequently, p_s reaches a maximum at different points in the cake and then decreases. Rigorous procedures require that the pressure reversal (Tiller and Horng, 1983) be considered in numerical calculations. However, with the cakes encountered in this investigation, the effect of reaching maximum values of p_s at different points in the cake affected less than 1.0% of the cake and has been neglected.

Experimental Volume vs. Time Data

Experimental results of V vs. t are illustrated in Figure 9 for systems of $CaCO_3$ with (1) water and (2) a water-glycerine solution. Figure 10 contains plots of dt/dv vs. v. The break-point corresponds to the end of particle deposition and the beginning of permeation of clear liquid. The interfaces of the clear liquid, r_L, and the clear liquid-slurry, r_s, were obtained photographically during the particle deposition and permeation processes and are shown in Figure 11. The cake surface could not be seen, and the r_c curve was calculated. The point at which the suspension disappears corresponds to the break point in Figure 10.

Pressure Distributions

Pressure distribution curves vary in accord with the existence of slurry and liquid layers above the cake. In Figure 12 the hydraulic pressure p_L, effective pressure p_s, and total pressure $p_T = p_s + p_L$ are illustrated for centrifugal filtration of 500 mL of an approximate 30 wt. % $CaCO_3$ in water. The conditions correspond generally to the region AB in Figure 4 and specifically to the time when 95 mL of filtrate had been produced. The total pressure is identical to the liquid pressure throughout the clear liquid and slurry regions along AB in Figure 12. The value of the liquid pressure at the cake surface is given by Eq. 35 and is represented by point B. At r_c, p_L begins to decrease and reaches p_1 at r_o. The effective pressure p_s is zero at r_c and rises to its maximum value at r_o.

After the slurry has disappeared and the cake ceases to grow, the remaining liquid must permeate through the cake, region BC of Figure 4, or be drained by means of a siphon from the centrifuge. The pressure distributions take the form shown in Figure 13. Inasmuch as the liquid level is decreasing, the pressure curves drop with time. The cake thickness remains constant because the p_s curves are successively lower as time passes. A

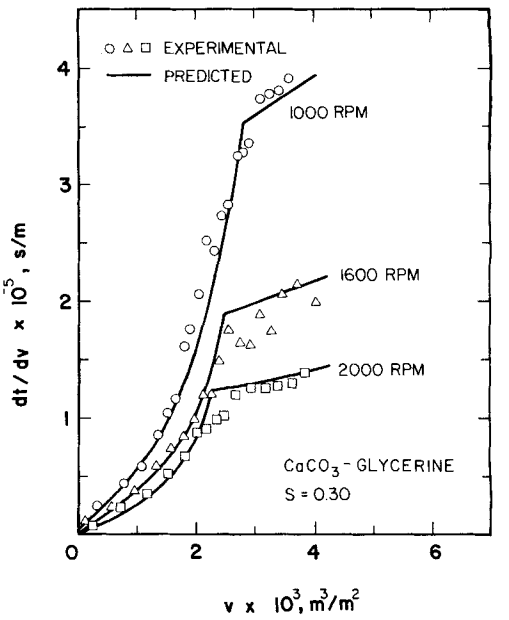

Figure 10. Experimental and predicted results, dt/dv vs. v.

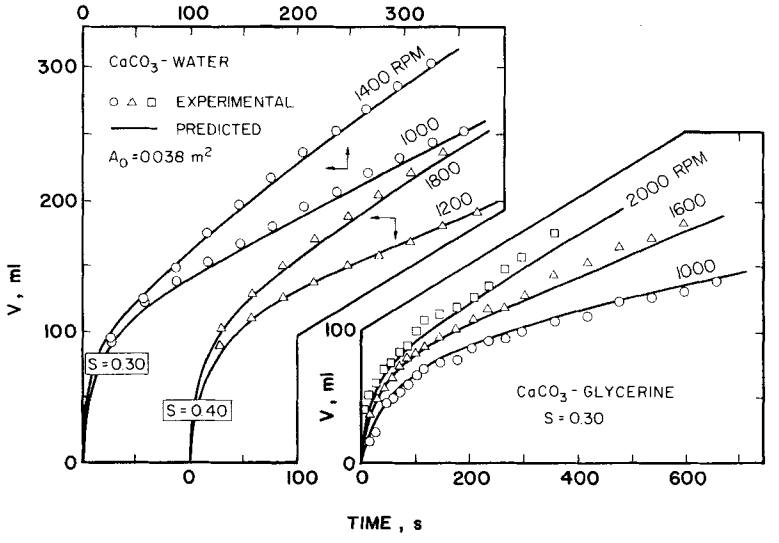

Figure 9. Experimental and predicted results, V vs. t.

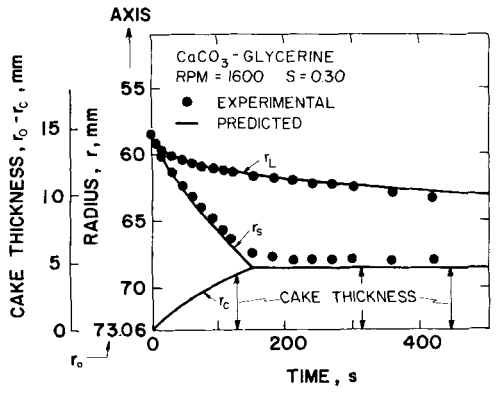

Figure 11. Experimental and predicted results, r_L, r_S, and r_C vs. t.

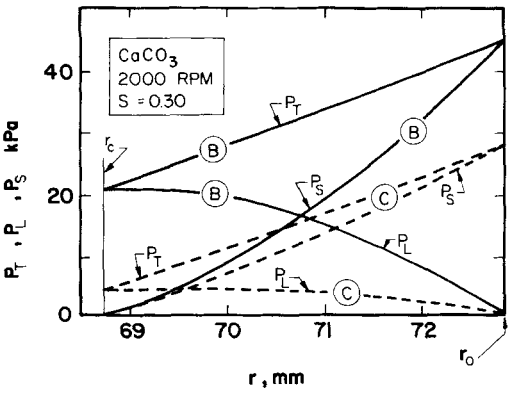

Figure 13. Pressure distributions in a cake, permeating period.

vertical line at $r = r_c$ indicates the constancy of the cake thickness. Curves marked B in Figure 13 correspond to the point B in Figure 4 where the particles in suspension have just disappeared. The curves designated by C represent conditions just prior to reaching point C in Figure 4.

The p_s curve marked B in Figure 13 lies above all successive effective pressures during the permeation period. Therefore, the cake structure does not change and the average values of alpha (or permeability) and porosity remain unchanged.

Comparison of Centrifugal and Constant-Pressure Filtration

Customarily, material coordinates are used in filtration rather than spatial coordinates. Unfortunately, the material coordinate equivalent of Eqs. 30 and 34 is algebraically complex and difficult to manipulate. Therefore, we shall employ an approximation to introduce the material coordinate, mass of dry solids per unit height, to replace the radius. The equations will be applied to thin cakes as used in this investigation. We begin by rewriting the Darcy Eq. 30

$$dp_L = \rho r\omega^2 dr - \frac{\mu r_o u_o}{rK}\, dr \tag{40}$$

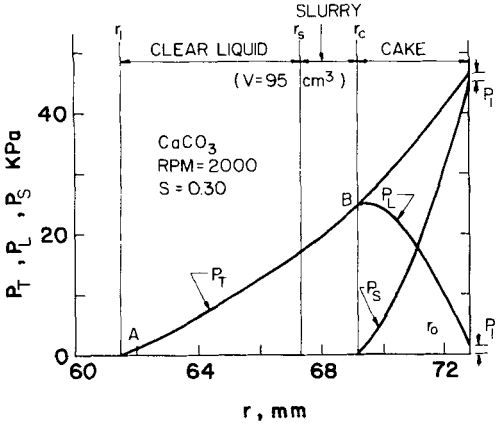

Figure 12. Pressure distributions in a cake, filtering period.

Integrating Eq. 40 from the cake surface where p_L is given by Eq. 35 to the medium where $p_L = p_1$ as given by Eq. 36 and simplifying yields

$$\frac{\omega^2}{2}\left[\rho(r_o^2 - r_c^2 + r_s^2 - r_L^2) + \rho_{sL}(r_c^2 - r_s^2)\right] = \mu u_o R_m + \mu r_o u_o \int_{r_c}^{r_o} \frac{dr}{Kr} \tag{41}$$

The quantity on the lefthand side represents the pressure drop Δp_L of the liquid over the cake and medium. The integral on the righthand side cannot be evaluated in its existing form as K is a function of p_s. However, an average can be defined as

$$\frac{r_o - r_c}{(Kr)_{av}} = \int_{r_c}^{r_o} \frac{dr}{Kr} \tag{42}$$

Substituting Eq. 42 for the integral in Eq. 41 and introducing the overall flow rate $Q = 2\pi r_o u_o$ leads to

$$r_o u_o = \frac{Q}{2\pi} = \frac{\Delta p_L}{\mu\left[\dfrac{r_o - r_c}{(Kr)_{av}} + \dfrac{R_m}{r_o}\right]} \tag{43}$$

We next divide by the arithmetic average of the radius $r_{av} = (r_o + r_c)/2$ and define the average flow rate as $Q = 2\pi r_{av} q_{av}$. We obtain

$$q_{av} = \frac{\Delta p_L}{\mu\left[\dfrac{r_o^2 - r_c^2}{2(Kr)_{av}} + \dfrac{r_{av}}{r_o} R_m\right]} \tag{44}$$

The mass of dry solids per unit area based on r_{av} is next introduced

$$w_c = \frac{W_c}{2\pi r_{av}} = \rho_s \epsilon_{av} \frac{r_o^2 - r_c^2}{r_o + r_c} \tag{45}$$

Substituting in Eq. 45 yields

$$q_{av} = \frac{\Delta p_L}{\mu\left[\dfrac{r_{av}w_c}{\rho_s\epsilon_{av}(Kr)_{av}} + \dfrac{r_{av}}{r_o}R_m\right]} \tag{46}$$

We now define K_{av} and α_{av}, the specific flow resistance, by

$$(Kr)_{av} = K_{av}r_{LM} \quad \alpha_{av} = 1/\rho_s\epsilon_{sav}K_{av} \tag{47}$$

Substituting in Eq. 47

$$q_{av} = \frac{\Delta p_L}{\mu\left[\alpha_{av}w_c\dfrac{r_{av}}{r_{LM}} + R_m\dfrac{r_{av}}{r_o}\right]} \tag{48}$$

In many centrifugal filtration operations, cakes are relatively thin and the ratio r_{av}/r_{LM} is nearly unity. Under such circumstances, the approximations proposed in Eq. 48 may be assumed to yield reasonable results.

Use of q_{av} suffers from calculations being based upon a changing area. Therefore, we choose to revert to utilization of rates based upon the outer radius and multiply Eq. 48 by r_{av}/r_o to produce

$$u_o = \frac{\Delta p_L}{\mu(\alpha_{av}W_c/A_e + R_m)} \tag{49}$$

where the effective area A_e is defined by

$$A_e = 2\pi r_{av}(r_{LM}/r_o) \tag{50}$$

In constant-pressure filtration, the governing flow rate equation is identical to Eq. 49 if A_e is identified with the constant cross-sectional area of a filter. However, appearances are deceptive, and pitfalls must be avoided in making comparisons between calculated values for constant-pressure filtration and centrifugation.

In one-dimensional, Cartesian coordinate filtration, α_{av} is assumed to be a unique function of the pressure drop across the cake. The α_{av} vs. Δp_c dependency is based upon the existence of a unique relationship between the effective pressure p_s and the fractional distance x/L through the cake. The usual simplifying assumptions employed in filtration lead to plots of p_s as a function of x/L that depend only on cake compressibility as reflected in the constitutive equations involving p_s and local values of α.

The p_s vs. r relation involved in centrifugal filtration is different from the corresponding p_s vs. x relationship in one-dimensional, Cartesian coordinate filtration; consequently, the average filtration resistance will not be the same even if the liquid pressure drop across the cake is the same.

In virtually all industrial and laboratory filtrations using vacuum, gas pressure, positive displacement, or centrifugal pumps for the driving force, the pressure drop across the cake increases with time. However, in batch centrifugal filtration the liquid level decreases with time, and Δp_L as obtained from Eq. 37 decreases as the quantity of liquid decreases and r_L increases. Decreasing the pressure drop across the cake leads to decreasing values of effective pressure. This in turn calls into play the principle of irreversibility in stress application to particulate beds. Porosity is assumed to be an irreversible function of the highest value of p_s reached at any time during a separation process. Stress distribution is affected by pressure reversal and further distorts the difference between cakes formed under conditions of constant pressure and centrifugal filtration.

Centrifugal filtration tests can be carried out in two different fashions. In one method, the cake is formed and then pure liquid is introduced into the centrifuge. Flow rates through the fixed mass are then studied as a function of rotational speed. This is the method recommended by Hultsch and Wilkesmann (1977). In the second method, which was used in this investigation, the volume of filtrate is obtained during the combined sedimentation and filtration period, in contrast to simply flowing liquid through a constant mass of cake. In this second method, serious calculational errors can be made if the mass of cake formed is based upon a material balance involving only the filtrate volume, as is customary in pressure filtration. A mass balance over slurry, cake, and filtrate yields

$$W_c' = \frac{\rho_s\epsilon_{sav}\phi_{sF}}{\epsilon_{sav} - \phi_{sF}}V \tag{51}$$

Ignored in this balance is the changing slurry concentration, Eq. 14, and the mass deposited due to sedimentation, Eq. 26. Average specific resistances will be too high if calculated on the basis of the volume of filtrate. Rushton (1970) and Rushton and Spear (1975) reported values of α_{av} obtained in centrifugal filtration to be higher than those resulting from constant-pressure filtration.

In Figure 14 plots of α_{av} vs. the volume filtered per unit area are shown as calculaed on the basis of the filtrate volume in strict accord with Eq. 51 and accounting for sedimentation of the solid particles. Experimental values of filtrate volume vs. time were obtained during centrifugation of a slurry of $CaCO_3$ in liquid consisting of 30% glycerol in water. The line marked W_c' represents the mass of dry solid calculated from Eq. 51. The mass calculated on the basis of the added sedimentation is shown as W_c. Point B in Figure 14 corresponds to B in Figure 4; it corresponds to the point where the particles in the suspension disappear leaving clear liquid above the cake. The W_c' and W_c lines would intersect at point C in Figure 4 where the supernatant liquid just disappears. Values of α_{av}' calculated on the basis

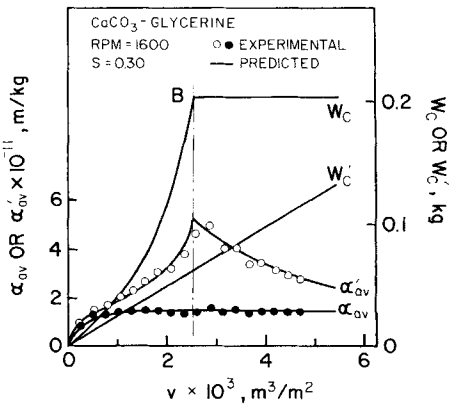

Figure 14. α_{av} and W_c calculated on the basis of filtrate volume and solid mass.

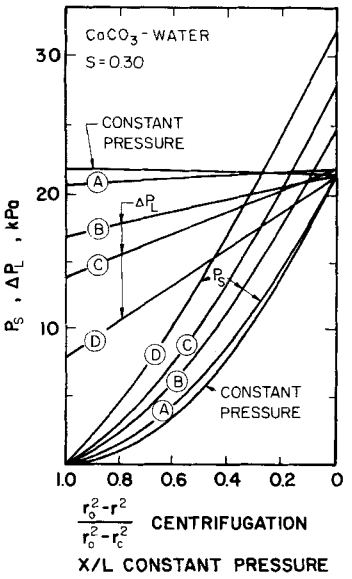

Figure 15. Comparison of pressure distributions in cakes of constant-pressure filtration and centrifugal filtration.

of W_c' are much larger than α_{av} as derived from the W_c vs. t curve.

As previously pointed out, the pressure drop on the liquid, Δp_L, in one-dimensional, Cartesian coordinate filtration equals the increase, Δp_s, in the effective pressure. Furthermore, the p_s, ϵ, and local alpha distributions are unique functions of the fractional distance through the cake for constant $\Delta p_c = \Delta p_L$. In centrifugal filtration, the p_s, ϵ, and α curves are not unique functions of Δp_s. The liquid driving force represented by Δp_c does not equal Δp_s, which determines the cake structure.

In Figure 15 calculated values are shown for the liquid pressure drop, Δp_L, and p_s as functions of position in cakes produced in both centrifugal (A–D) and constant-pressure filtration. The differing p_s curves lead to different cake structures and average flow resistances. Conditions were chosen so that the liquid driving force, Δp_L, in the centrifugal processes approximated the value of Δp_c in the constant-pressure filtration. As can be seen, the p_s distributions vary widely as do the average flow resistances. In order to correlate the data, we have chosen to use an average value of the effective pressure, $\bar{p}_s$, rather than a difference such as Δp_c. The p_s at any point in the cake is weighted by the volume V_F over which it is effective, and is defined by

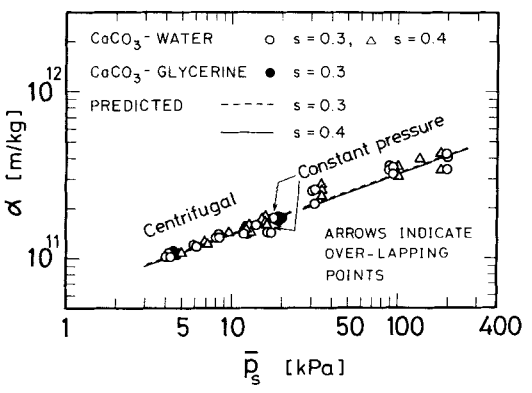

Figure 16. Experimental and predicted results for centrifugal and constant-pressure filtration, α_{av} vs. $\bar{p}_s$.

Table 1. Comparison of Centrifugal and Constant-Pressure Filtration

Process	Pressure, kPa Δp_L	Δp_c	$\bar{p}_s$	ϵ_{sav}	α_{av} (m/kg)
Constant-pressure	21.6	21.6*	7.36	0.407	1.26 (10^{11})
Centrifugal					
A	22.0	19.9	7.82	0.416	1.30 (10^{11})
B	21.5	20.5	9.86	0.429	1.42 (10^{11})
C	21.9	20.9	11.68	0.436	1.50 (10^{11})
D	21.4	20.8	14.42	0.446	1.70 (10^{11})

*R_m assumed to be zero

$$\bar{p}_s = \frac{1}{V_{FT}} \int_o^{V_{FT}} p_s dV_F \tag{52}$$

where V_{FT} is the total volume occupied by the cake. In constant-pressure filtration

$$\bar{p}_s = \frac{1}{L} \int_o^L p_s dx \tag{53}$$

and in centrifugal filtration

$$\bar{p}_s = \frac{1}{r_o^2 - r_c^2} \int_o^{r_o^2 - r_c^2} p_s d(r_o^2 - r^2) \tag{54}$$

The abscissa in Figure 16 has been chosen in accord with Eqs. 53 and 54. Results of the calculations are shown in Table 1.

In Figure 16 a plot of average alpha is shown for both centrifugal and constant-pressure filtration as a function of $\bar{p}_s$. The slope is 0.36, and the data fall on a single line. Two of the constant-pressure filtrations were carried out in the low range involved in the centrifugal filtration.

Acknowledgment

Experimental work and numerical calculations were performed in the laboratories of Yamaguchi University. Masao Sambuichi thanks the Ministery of Education (Japan) for supporting a visit to the Chemical Engineering Department of the University of Houston during 1982–1983 and for Grant Nos. R34-503528 and 56035022. Frank M. Tiller thanks the Office of Basic Energy Sciences of the U.S. Department of Energy for Grant No. DE-AS05-81ER-10946 covering fundamental investigations in solid-liquid separation. The authors wish to thank Ube Industries Ltd. for the materials used in this experiment.

Notation

A_e = effective filtration area, m²
A_o = filtration area at filter medium, m²
c_1, c_2 = constants, Eq. 13, m/s
F_s = stress/height on particles at radius r, N/m
g = gravitational acceleration, 9.807 m/s²
h = height of cylindrical filter surface, m
k_o = ratio of lateral stress to normal stress
K = local permeability, m²
K_{av} = average permeability, m²
L = cake thickness, m

p_L = hydraulic pressure, Pa
p_{Lc} = hydraulic pressure at cake surface, Pa
p_s = solid compressive pressure, Pa
$\bar{p}_s$ = average compressive pressure, Eq. 52, Pa
p_T = total pressure, $p_s + p_L$, Pa
p_1 = hydraulic pressure at medium, Pa
Δp_c = hydraulic pressure drop across cake, Pa
Δp_L = hydraulic pressure drop aross cake and medium, Pa
Δp_m = hydraulic pressure drop across filter medium, Pa
Δp_s = increase in effective pressure across cake, Pa
Q = total flow rate of filtrate per unit height, $m^3/m \cdot s$
q = superficial flow rate at r, m/s
q_{av} = average superficial flow rate, m/s
r = radius, m
r_{av} = arithmetic average of cake radius, m
r_c = radius of cake surface, m
r_F = radius of liquid surface at $t = 0$, m
r_L = radius of a clear liquid surface, m
r_{LM} = logarithmic mean of cake radius, m
r_o = centrifuge bowl radius, m
r_s = radius of a slurry-supernatant interface, m
r_1, r_2 = arbitrary value of r in slurry, m
R_m = resistance of a filter medium, 1/m
s = mass fraction of solids in slurry
t = time, s
u = upward liquid velocity balanced for settling solids, m/s
u_c = settling velocity of slurry-supernatant interface in a sedimenting centrifuge, m/s
u_g = settling velocity of slurry-supernatant interface in a gravitational field, m/s
u_o = flow rate of filtrate at r_o per unit area, m/s
u_s = settling velocity of slurry-supernatant interface in a filtering centrifuge, m/s
v = volume of filtrate per unit area of filter medium, m^3/m^2
V = total volume of filtrate, m^3
V_F = volume of cake between medium and arbitrary point in cake, m^3
V_{FT} = total cake volume, m^3
w_c = mass of solid per unit area, kg/m^2
W_c = total mass of solid in centrifugal cake, kg
W'_c = total mass of solid calculated on the basis of filtrate, Eq. 51, kg
x = distance from bottom in gravity sedimentation, m

Greek letters

α = local value of specific resistance of cake, m/kg
α_{av} = average specific resistance of cake, m/kg
α'_{av} = average specific resistance based on Eq. 51, m/kg
α_i = value of α when $p_s \leq 23.5$ Pa, Pa
ϵ = local value of porosity
ϵ_{av} = average porosity of cake
ϵ_i = value of ϵ when $p_s \leq 23.5$ Pa
ϵ_s = local value of solid fraction, $1 - \epsilon$
ϵ_{sav} = average solid fraction of cake
ϵ_{so} = value of ϵ_s under null load
θ = angle, rad
μ = viscosity of filtrate, Pa · s
ρ = density of filtrate, kg/m^3
ρ_s = true density of solid particles, kg/m^3
ρ_{sL} = density of slurry, kg/m^3
ϕ = volume fraction of liquid
ϕ_s = volume fraction of solid
ϕ_{sF} = initial volume fraction of solid in slurry
ω = angular velocity, rad/s

Literature Cited

Brown, T. J., *An Introduction to Ultracentrifugation,* Wiley, New York, 50 (1970).

Dunn, I. S., L. R. Anderson, and F. W. Kiefer, *Geotechnical Analysis,* Wiley, New York, 113 (1980).

Fujita, H., *Mathematical Theory of Sedimentation Analysis,* Academic Press, New York (1962).

Grace, H. P., "Resistance and Compressibility of Filter Cakes," *Chem. Eng. Prog.,* **49,** 303, 367, 427 (1953).

Hultsch, G., and H. Wilkesmann, "Filtering Centrifuges," *Solid-Liquid Separation Equipment Scale-Up,* D. Purchas, ed., Uplands Press, Croydon, England (1977).

Kamac, H. J., "Particle Size Determination by Centrifugal Pipet Sedimentation," *Anal. Chem.,* **23,** 844 (1951).

Kynch, G. J., "A Theory of Sedimentation," *Trans. Faraday Soc.,* **48,** 166 (1952).

Lilley, K., and G. Hultsch, "Upgrading Centrifuge Performance by the Siphon Effect," *Filtration and Separation,* **12,** 70 (1975).

Oyama, Y., and S. Sumikawa, "On the Fundamental Study of Centrifugal Filtration," *Kagaku Kogaku (J. Chem. Eng. Japan),* **18,** 593 (1954).

Risbud, H. M., "Mechanical Expression, Stresses at Cake Boundaries and New CP Cell," Ph.D. Diss., Univ. Houston, TX (1974).

Rushton, A., "The Behavior of Filter Cloths in Centrifugation," *Filtration and Separation,* **7,** 286, 318 (1970).

Rushton, A., and M. Spear, "Centrifugal Filtration and Permeation," *Filtration and Separation,* **12,** 254 (1975).

Ruth, B. F., "Correlating Filtration Theory with Industrial Practice," *Ind. Eng. Chem.,* **38,** 564 (1946).

Sambuichi, M., H. Nakakura, K. Saitoh, and K. Osasa, "Experimental Study on Batchwise Centrifugal Filtration," Prepr. 45th Ann. Meet. Soc. Chem. Eng. Japan, E301–302 (1980).

Sambuichi, M., H. Nakakura, and K. Osasa, "The Effect of Gravity Settling on Constant-Pressure Filtrations," *Mem. Fac. Eng., Yamaguchi Univ.,* **33,** 65 (1982).

Shirato, M., and T. Aragaki, "The Relation between Hydraulic and Compressive Pressure in Non-Unidimensional Filter Cakes," *Kagaku Kogaku,* **33,** 205 (1969).

Shirato, M., personal communication (1983).

Shirato, M., H. Kato, K. Kobayashi, and H. Sakazaki, "Analysis of Settling of Thick Slurries Due to Consolidation," *J. Chem. Eng. Japan,* **3,** 98 (1970).

Straumann, R., "Einfluss der Sedimentation auf die Filtration," *Chem. Ing. Tech.,* **35,** 715 (1963).

Tiller, F. M., "Revision of Kynch Sedimentation Theory," *AIChE J.,* **27,** 823 (1981).

Tiller, F. M., and L. L. Horng, "Hydraulic Deliquoring of Compressible Filter Cakes. I: Reverse Flow in Fileer Presses," *AIChE J.,* **29,** 297 (1983).

Tiller, F. M., and W. F. Leu, "Basic Data-Fitting in Filtration," *J. Chinese Inst. Chem. Eng.,* **11,** 61 (1980).

Tiller, F. M., S. Haynes, and W. M. Lu, "The Role of Porosity in Filtration. VII: Effect of Side-wall Friction in Compression-Permeability Cells," *AIChE J.,* **18,** 13 (1972).

Valleroy, V. V., and J. O. Maloney, "Comparison of the Specific Resistances of Cakes Formed in Filters and Centrifuges," *AIChE J.,* **6,** 382 (1960).

Wakeman, R. J., and R. G. Holdrich, "Theoretical and Experimental Modeling of Solids and Liquid Pressures in Batch Sedimentation," *World Filtration Cong. III,* Uplands Press, Croydon, England, **1,** 346 (1982).

Willis, M. S., and I. Tosun, "A Rigorous Cake Filtration Theory," *Chem. Eng. Sci.,* **35,** 2427 (1980).

Manuscript received Oct. 7, 1985, and revision received July 29, 1986.